Title: A missense TGFB2 variant p.(Arg320Cys) causes a paradoxical and striking increase in Aortic TGFB1/2 expression

Raya Al Maskari[1], Yasmin[1], Sarah Cleary[1], Nikki Figg[1], Sarju Mehta[2], Doris Rassl[3], Ian Wilkinson[1] and Kevin M O'Shaughnessy[1]

[1] Department of Medicine (EMIT and CVD divisions), University of Cambridge, UK; [2] Medical Genetics, Addenbrookes Hospital, UK; [3] Pathology, Papworth Hospital, UK

Running title: LDS4 p.(Arg320Cys) mutation increases TGFβ signaling

Corresponding author: Kevin O'Shaughnessy (kmo22@medschl.cam.ac.uk)
Department of Medicine (EMIT Div)
Box 110, Level 6 ACCI
Addenbrookes Hospital
Cambridge CB2 2QQ, UK
E – kmo22@medschl.cam.ac.uk
P – 44 1223 762578

Conflict of interest: None

Abstract

Loeys-Dietz syndrome (LDS) is an autosomal dominant connective tissue disorder with a range of cardiovascular, skeletal, craniofacial and cutaneous manifestations. LDS type 4 is caused by mutations in TGFβ ligand 2 (TGFB2) and based on the family pedigrees described to date, appears to have a milder clinical phenotype, often presenting with isolated aortic disease. We sought to investigate its molecular basis in a new pedigree. We identified a missense variant p.(Arg320Cys) (NM_003238.3) in a highly evolutionary conserved region of TGFB2 in a new LDS type 4 pedigree with multiple cases of aortic aneurysms and dissections. There was striking up-regulation of TGFB1 and TGFB2 expression on immunofluorescent staining and western blotting of the aortic tissue from the index case confirming the functional importance of the variant. This case highlights the striking paradox of predicted loss-of-function mutations in TGFB2 causing enhanced TGFβ signaling in this emerging familial aortopathy.

Keywords: Loeys-Dietz Syndrome LDS4, TGFB2 mutation, Aortic Aneurysm/Dissection

Introduction

Loeys-Dietz syndrome (LDS) is an inherited autosomal dominant (AD) systemic disorder with a broad phenotypic spectrum of cardiovascular, skeletal, craniofacial and cutaneous manifestations (OMIM #609192). The hallmark of early and progressive aortic root dilatation, predisposes to premature death from dissection and rupture of the aorta [1]. Other classic features include widespread arterial tortuosity, bicuspid aortic valve, bifid uvula/cleft palate and hypertelorism [1]. LDS is caused by disruption to the transforming growth factor beta (TGFβ) signaling pathway. TGFβ proteins regulate key processes including cell proliferation, angiogenesis and matrix turnover by signaling through serine/threonine kinase receptors (TGFBR1, TGFBR2) and downstream effectors, the SMAD proteins [2]. TGFβ is synthesized as a dimer bound to a latency associated peptide (LAP) that prevents the cytokine from binding to its receptors [3]. Complex mechanisms also control TGFβ sequestration and release by the extracellular matrix (ECM) [3].

Mutations in TGFBR1, TGFBR2, TGFβ ligands 2 and 3 (TGFB2, TGFB3) and SMAD3 are associated with LDS disease pathogenesis [4-7]. Precise genotype-phenotype correlations are still lacking, but it is proposed that a mutation in any of these genes plus arterial aneurysm/dissection or a family history of LDS is sufficient for the diagnosis [8]. LDS type 4 is caused by mutations in TGFB2 and represents a milder end of the LDS spectrum often with isolated aortic disease presenting in the mid-thirties [9]. To date, less than 20 mutations in TGFB2 have been identified usually in the LAP domain of the protein [6, 9-13]. However, the underlying pathogenic mechanisms remain unclear. Most of the mutations are predicted to be

loss-of-function, but their downstream effect appears to be a paradoxical activation of TGFβ signaling [14].

Here we report a new pedigree with LDS4 and confirm that the causative variant p.(Arg320Cys) (NM_003238.3) causes striking upregulation of TGFB1/2 expression in the aorta. This confirms that the variant is functional and corroborates previous reports of an enhanced aortic TGFβ "tissue signature" in LDS and other TGFβ vasculopathies.

Materials and Methods

Data Submission

Phenotype and variant data were submitted into LOVD v.3.0 Build 16 http://medgen.ua.ac.be/LOVDv.3.0/individuals/00000322.

Control Subjects

Formalin-fixed and paraffin embedded (FFPE) aortic tissue from age and gender matched donors (n=5) were obtained from the Transplant service at Addenbrooke's Hospital (Cambridge, UK). All samples were handled in accordance with the policies and procedures of the Human Tissue Act and had Local and Regional Ethics approval.

Immunofluorescence staining

FFPE sections of the surgical specimen were deparaffinised in Histoclear (National Diagnostics, Atlanta, GA, USA) then dehydrated through graduated methanols. Antigen retrieval was performed in pH6 citrate buffer (Vector Laboratories Ltd, Peterborough, UK) using 2100 Retriever (Aptum Biologics Ltd, Southampton, UK). Sections were permeabilised with 0.05% v/v Triton X-100–PBS for 5 min and

blocked for 2 h at room temperature with 5% v/v goat serum in 0.05% v/v Triton™ X-100–PBS. Sections were probed with mouse monoclonal to TGFB2 (Abcam, Cambridge, UK) and mouse monoclonal to TGFB1 (Abcam) for 16 h at 4°C at 1:200 dilution in 2% v/v goat serum in 0.05% v/v Triton™ X-100–PBS. Slides were then washed for 5 min in 0.05% v/v Triton™ X-100–PBS and incubated in secondary antibody for 1 h at room temperature. Pre-absorbed goat IgG-conjugated Alexa Fluor® 633 secondary antibody (ThermoFisher Scientific, Waltham, MA, USA) was used at 1:200 dilution in 2% v/v goat serum in 0.05% v/v Triton™ X-100–PBS. Sections were counterstained with Sytox® Orange (ThermoFisher Scientific) at 1/10,000 in Milli-Q® water for 20 min at room temperature then mounted with ProLong® Gold Antifade Mountant (ThermoFisher Scientific).

Images were acquired with a Leica SP8 (Leica Microsystems, Wetzlar, Germany) inverted laser scanning confocal microscope using a 20X 1.4 N.A. dry objective. Acquisition parameters were: 12-bit, 1024 x 1024 pixels, 1.25x and 3x digital zooms, 8000 Hz scan speed, 16-line Kalman filtering and 2 frame accumulation. All images were acquired using identical scan settings.

Protein Extraction and Western blotting

Western blotting for TGFB1 and TGFB2 was performed in the case and two of the controls. Three 15μm FFPE sections of each tissue sample were deparaffinised in Histoclear® 3 times. The procedure was serially repeated with 100%, 95% and 70% ethanol, washing twice for 10 min each. Pellets were air dried, re-suspended in Extraction Buffer EXB Plus (Qiagen, Hilden, Germany) containing β-mercaptoethanol and incubated at 4°C for 5 min then at 100°C for 20 min followed by a 2 h incubation at 80°C with agitation and a final incubation at 4°C for 1 min.

Samples were then centrifuged at 4°C for 15 min and the protein quantified using Pierce™ BCA protein assay (ThermoFisher Scientific) and stored at -70°C until further use.

Ten µg of protein lysates were used for the western blot. Samples were incubated at 70°C for 10 min in Lithium dodecylsulfate (LDS) sample loading buffer (ThermoFisher Scientific) and Bolt® sample reducing agent (ThermoFisher Scientific). Samples for TGFB1 blotting were performed under non-reducing conditions. Protein was separated by SDS-gel electrophoresis in 4-12% gradient Bis-Tris Plus Bolt® gels (ThermoFisher Scientific) at 200V for 30 min and transfered to 0.22µM nitrocellulose membrane (ThermoFisher Scientific) using the iBlot2 dry blotting system (ThermoFisher Scientific) at 20V for 10 min. Prior to transfer, gels were equilibrated for 5min in NuPage transfer buffer (ThermoFisher Scientific) containing 10% methanol. Membranes were blocked with 5% w/v milk in TBS buffer for 1 h at room temperature then incubated with primary antibodies in 5% milk w/v in 0.1% v/v Tween® 20-TBS for 16 h at 4°C. Anti-TGFB2 (Abcam) rabbit polyclonal IgG antibody was used at 1:500 dilution and β-actin mouse monoclonal IgG (ThermoFisher Scientific) was used as a loading control at 1:1000 dilution. Anti-TGFB1 (Abcam) mouse monoclonal IgG antibody was used at 1:500 dilution and β-actin rabbit polyclonal IgG (Sigma Aldrich, St Louis, MO, USA) was used as a loading control at 1:1000 dilution. Secondary antibodies were incubated in 0.1% v/v Tween® 20-TBS for 1 h at room temperature. Donkey anti-rabbit (LI-COR Biotechnology UK Ltd, Cambridge, UK) IRDye® 800CW and goat anti-mouse (ThermoFisher Scientific) Alexa Fluor® 680 conjugated secondary antibodies were used at 1:5000 dilution. Membranes were washed in 0.1% v/v Tween® 20-TBS 3 times for 15 min each between primary and secondary antibody incubations and

before visualization. Protein bands were detected using the LI-COR Odessey system. Signal intensities were normalised against β-actin and quantified using ImageStudioLite software.

Results

Pedigree discovery

A 27-year-old man presented with severe pain radiating down his back after lifting a lawn mower into a van. The family history revealed several family members with aortic aneurysms and dissections: his mother (III:6) died following an aortic dissection, a maternal uncle (III:1) had emergency repair of an aortic aneurysm and his maternal grandfather (II:3) had a dissection of an abdominal aortic aneurysm and separate iliac artery aneurysms (Figure 1A). On examination, the only sign was an elevated BP of 240/100 mmHg. A CT scan with contrast showed a Stanford type-A dissection with an intimal flap extending the full length of the aorta from the aortic valve into both iliac arteries (Figure 1B). He underwent open aortic repair and a surgical specimen was recovered for further examination. Histologic examination showed fragmentation and disruption of the aortic elastic fibers and cystic medial necrosis (Figure 1C).

Sequencing and variant identification

DNA sequencing from the peripheral blood of the index case identified a missense variant (c.958C>T) (NM_003238.3) in exon 6 of the TGFB2 gene (NG_027721.1). This variant causes a p.(Arg320Cys) substitution in a highly conserved region of

TGFB2 (Figure 1D). The variant was also detected in the uncle (III:1) and two currently asymptomatic teenage family members (IV:3) and (IV:5).

TGFB1 and TGFB2 expression in the aorta

Immunofluorescent imaging showed markedly enhanced TGFB1 and TGFB2 expression in the aorta of the index case compared to age and gender-matched controls (Figure 2 and 3). This was confirmed by immunoblotting for both proteins in the aorta of IV:10 versus controls where the upregulation of TGFB1 was particularly striking (Figure 2 and 3).

Discussion

The p.(Arg320Cys) substitution is in a highly evolutionarily conserved region of TGFB2 and has a strong *in silico* prediction for pathogenicity [11]. However, there has been no evidence to confirm its functional effects [11]. We show for the first time that this variant does induce striking up-regulation of both TGFB1 and TGFB2 in the vessel wall of a subject with the variant. While this is unexplained by a loss-of-function variant in TGFB2, this signature of enhanced TGFβ signaling is believed to play a central role in the aortic dilatation and aneurysms seen in LDS, Marfan syndrome and other inherited aortopathies[15].

Of note, haploinsufficient $TGFB2^{+/-}$ mice develop aortic root dilatation and aneurysm and have a higher expression of phosphorylated SMAD2/3 and extracellular signal-regulated kinases (ERK1/2), indicating up-regulation of the TGFβ canonical (SMAD dependent) and non-canonical (SMAD independent) pathways [6]. The canonical pathway is involved in stimulating elastin and collagen while

repressing ECM degradation by inducing endogenous tissue inhibitor of metalloproteinases 1 and 3. These changes disrupt the normal architecture of the vessel wall [2]. Less is known about the role of the non-canonical pathway, however enhanced ERK activity appears to stimulate the expression of matrix metalloproteinases 2 and 9 to stimulate matrix degradation [2, 15].

Another suggestion to resolve the TGFβ vascular paradox, posits that other TGFB ligands are overexpressed to compensate for haploinsufficiency of a given TGFB ligand. This shift in ligand usage is seen with higher TGFB1 expression in $TGFB2^{+/-}$ mice [6] and in our index case. The high TGFB1/2 expression may even be a "repair process" by mesenchymal cells following damage to ECM [3].

As aortic aneurysm and dissection may be the only manifestation of LDS4, identifying family members with the variant is crucial for surveillance to improve clinical outcome. The striking activation of TGFβ signaling in these patients also suggests this may be a future therapeutic target for LDS.

Acknowledgements

Raya Al Maskari has a PhD studentship funded by the Omani government.

Conflict of interest: The authors declare no conflict of interest.

Author contributions

RAM, Y, SC and NF did the bench work; RAM did all the confocal imaging and blotting; SM provided medical genetics diagnostics and advice; DZ provided pathology services and advice; IB identified the pedigree and gave clinical advice; KMO conceived and ran the project and wrote the manuscript with RAM.

References

1. Loeys BL, Dietz HC. Loeys-Dietz Syndrome. In: Pagon RA AM, Ardinger HH, et al, editors., ed. *GeneReviews® [Internet]*. University of Washington, Seattle: Seattle (WA) 2013.
2. Jones JA, Spinale FG, Ikonomidis JS. Transforming growth factor-beta signaling in thoracic aortic aneurysm development: a paradox in pathogenesis. *J Vasc Res* 2009; **46**:119-137.
3. Horiguchi M, Ota M, Rifkin DB. Matrix control of transforming growth factor-beta function. *J Biochem* 2012; **152**: 321-329.
4. Loeys BL, Chen J, Neptune ER*, et al.* A syndrome of altered cardiovascular, craniofacial, neurocognitive and skeletal development caused by mutations in TGFBR1 or TGFBR2. *Nat Genet* 2005; **37**: 275-281.
5. van de Laar IM, Oldenburg RA, Pals G*, et al.* Mutations in SMAD3 cause a syndromic form of aortic aneurysms and dissections with early-onset osteoarthritis. *Nat Genet* 2011; **43**: 121-126.
6. Lindsay ME, Schepers D, Bolar NA*, et al.* Loss-of-function mutations in TGFB2 cause a syndromic presentation of thoracic aortic aneurysm. *Nat Genet* 2012; **44**: 922-927.
7. Bertoli-Avella AM, Gillis E, Morisaki H*, et al.* Mutations in a TGF-beta ligand, TGFB3, cause syndromic aortic aneurysms and dissections. *J Am Coll Cardiol* 2015; **65**: 1324-1336.
8. MacCarrick G, Black JH, 3rd, Bowdin S*, et al.* Loeys-Dietz syndrome: a primer for diagnosis and management. *Genet Med* 2014; **16**: 576-587.
9. Boileau C, Guo DC, Hanna N*, et al.* TGFB2 mutations cause familial thoracic aortic aneurysms and dissections associated with mild systemic features of Marfan syndrome. *Nat Genet* 2012; **44**: 916-921.
10. Ritelli M, Chiarelli N, Dordoni C*, et al.* Further delineation of Loeys-Dietz syndrome type 4 in a family with mild vascular involvement and a TGFB2 splicing mutation. *BMC Med Genet* 2014; **15**: 91.
11. Gago-Diaz M, Blanco-Verea A, Teixido-Tura G*, et al.* Whole exome sequencing for the identification of a new mutation in TGFB2 involved in a familial case of non-syndromic aortic disease. *Clin Chim Acta* 2014; **437**: 88-92.
12. Leutermann R, Sheikhzadeh S, Brockstadt L*, et al.* A 1-bp duplication in TGFB2 in three family members with a syndromic form of thoracic aortic aneurysm. *Eur J Hum Genet* 2014; **22**: 944-948.
13. Renard M, Callewaert B, Malfait F *et al.* Thoracic aortic-aneurysm and dissection in association with significant mitral valve disease caused by mutations in TGFB2. *Intern J Cardiol* 2013; **165**: 584-587.
14. Akhurst RJ. The paradoxical TGF-beta vasculopathies. *Nat Genet*: 2012; **44**: 838-839.
15. Lindsay ME, Dietz HC. Lessons on the pathogenesis of aneurysm from heritable conditions. *Nature* 2011; **473**: 308-316.

Titles and legends to figures

Figure 1 Clinical and Molecular Findings A. Family pedigree with multiple cases of aneurysms and dissections suggesting autosomal dominant inheritance. The variant was detected in the index case (IV:10) and III:1, IV:3 and IV:5. **B.** CT images showing an intimal flap (red arrows) extending from the aortic valve into the thoracic aorta. **C.** Elastin staining of IV:10 aorta showing extensive elastic fibre fragmentation at the site of dissection (scale bar=6mm). **D.** Sequencing chromatogram showing a missense mutation (c.958C>T) in exon 6 of TGFB2. The mutation is in a region of TGFB2 that is highly conserved across species. SP; signal peptide, LAP; latency-associated-peptide.

Figure 2 Aortic Expression of TGFB2 A. Western blots of aortic TGFB2 expression in IV:10 compared to two age-matched controls, TS218 and TS199. Signal intensities of TGFB2 normalized against β Actin indicate a twofold higher expression of TGFB2 in the mutant sample. **B.** Immunofluorescent staining of TGFB2 (green) shows increased expression in the aortic wall of IV:10 compared to TS218 and TS199. Elastic fibres appear as blue (autofluorescence) and nuclei are counterstained red (scale bar=50uM and the right-hand images are zoomed).

Figure 3 Aortic Expression of TGFB1 A. Western blots of aortic TGFB1 expression in IV:10 compared to two age-matched controls, TS218 and TS199. Signal intensities of TGFB1 normalized against β Actin indicate a 15-fold higher expression of TGFB1 in the mutant sample. **B.** Immunofluorescent staining of TGFB1 (green) shows increased expression in the aortic wall of IV:10 compared to TS218 and TS199. Elastic fibres appear as blue (autofluorescence) and nuclei are counterstained red (scale bar=50uM and the right-hand images are zoomed).

Figure 1

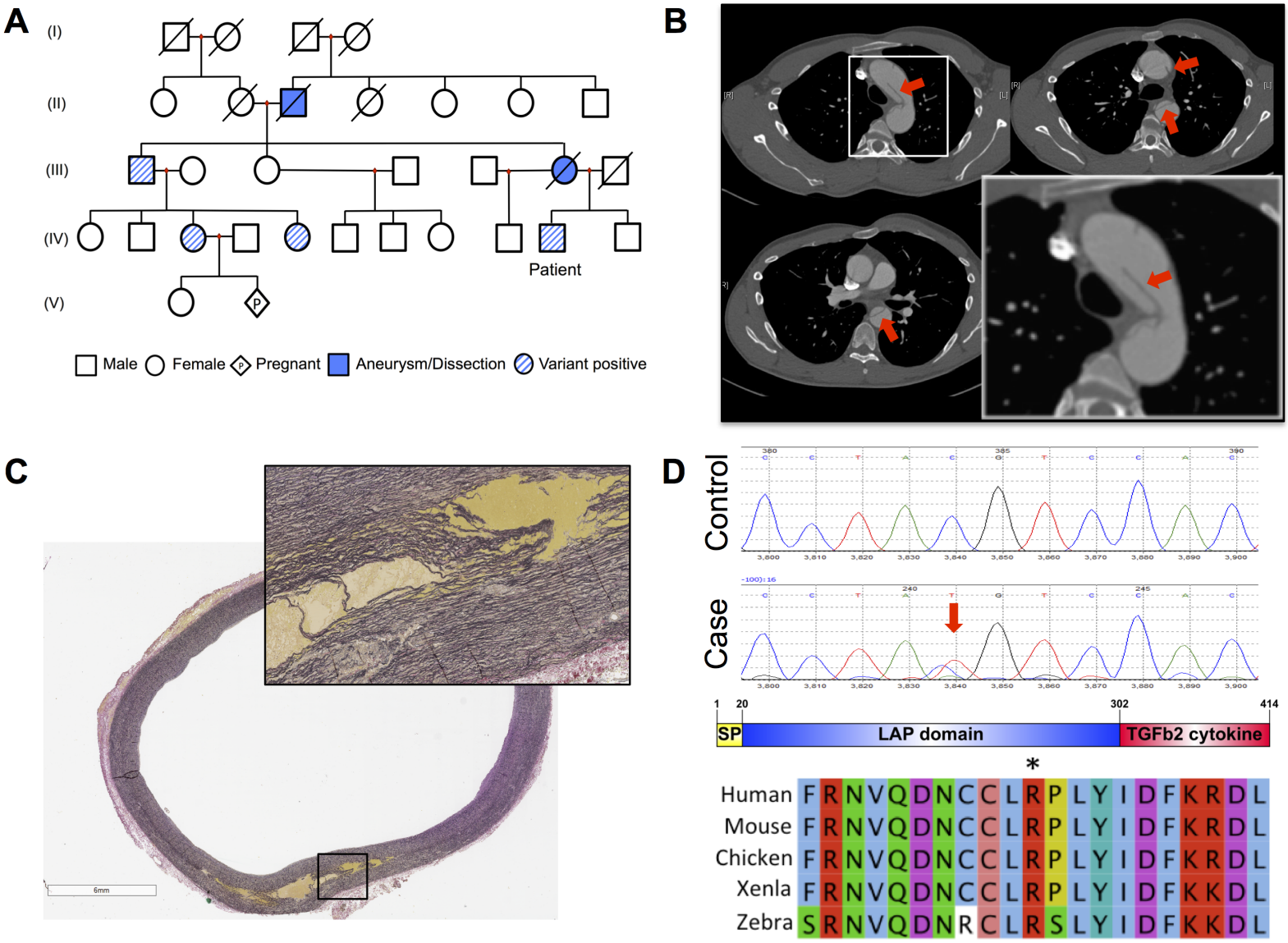
A
(I)
(II)
(III)
(IV)
(V)
Patient
P
Male
Female
Pregnant
Aneurysm/Dissection
Variant positive
B
C
6mm
D
Control
Case
SP
LAP domain
TGFb2 cytokine
1
20
302
414
*
Human F R N V Q D N C C L R P L Y I D F K R D L
Mouse F R N V Q D N C C L R P L Y I D F K R D L
Chicken F R N V Q D N C C L R P L Y I D F K R D L
Xenla F R N V Q D N C C L R P L Y I D F K K D L
Zebra S R N V Q D N R C L R S L Y I D F K K D L

Figure 2

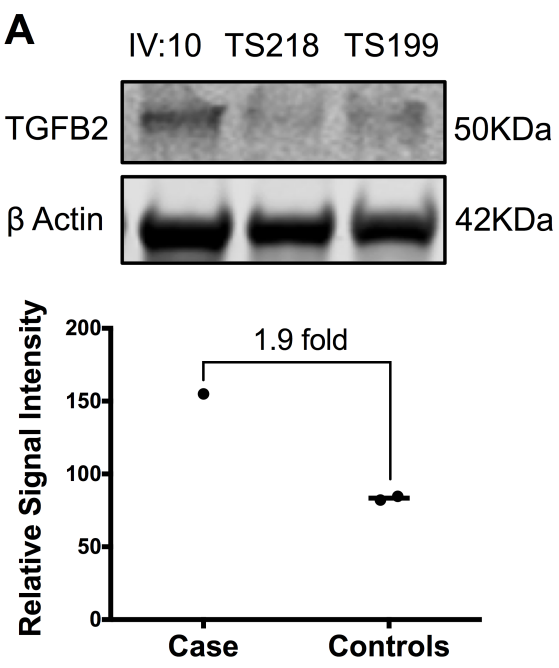
A
IV:10 TS218 TS199
TGFB2
50KDa
β Actin
42KDa
Relative Signal Intensity
200
150
100
50
0
1.9 fold
Case
Controls

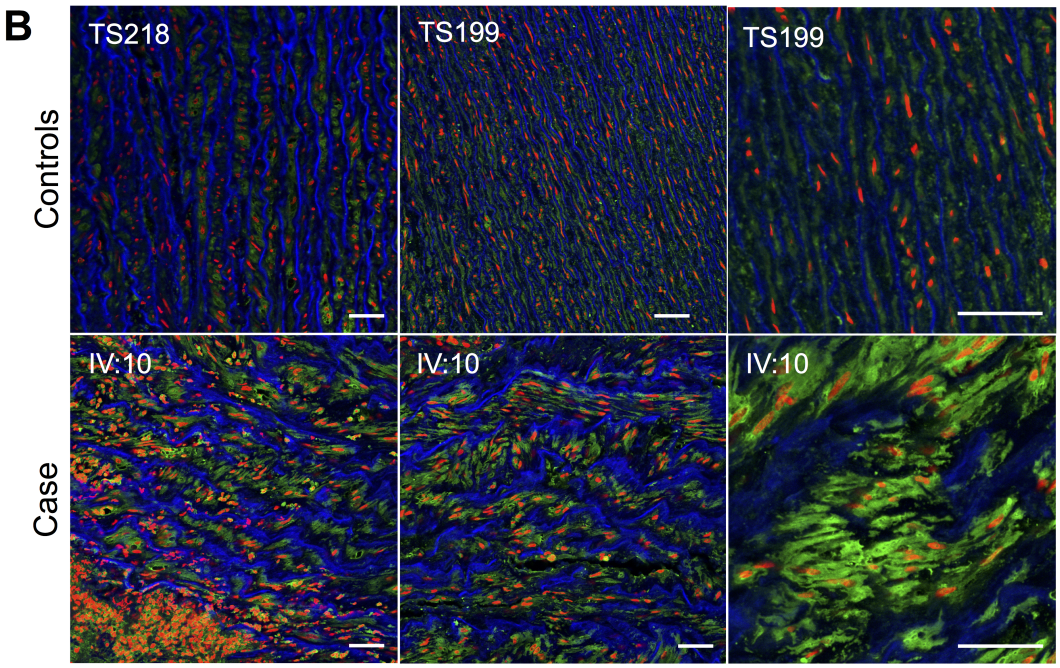
B
TS218
TS199
TS199
Controls
IV:10
IV:10
IV:10
Case

Figure 3

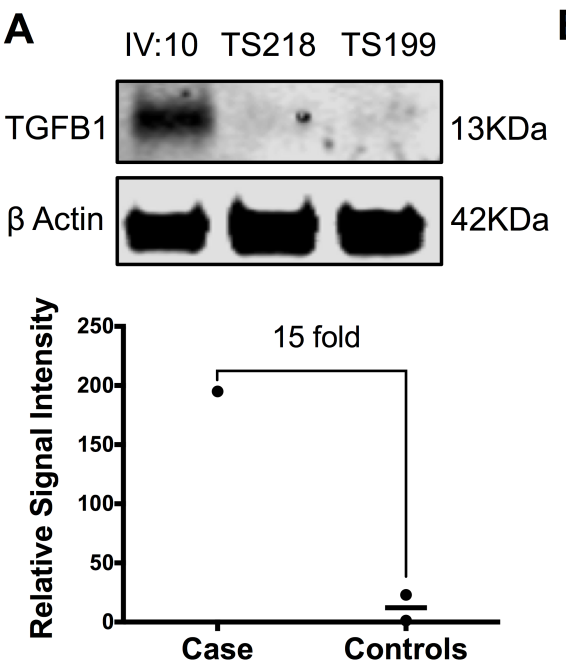
A
IV:10
TS218
TS199
TGFB1
13KDa
β Actin
42KDa
Relative Signal Intensity
250
200
150
100
50
0
15 fold
Case
Controls

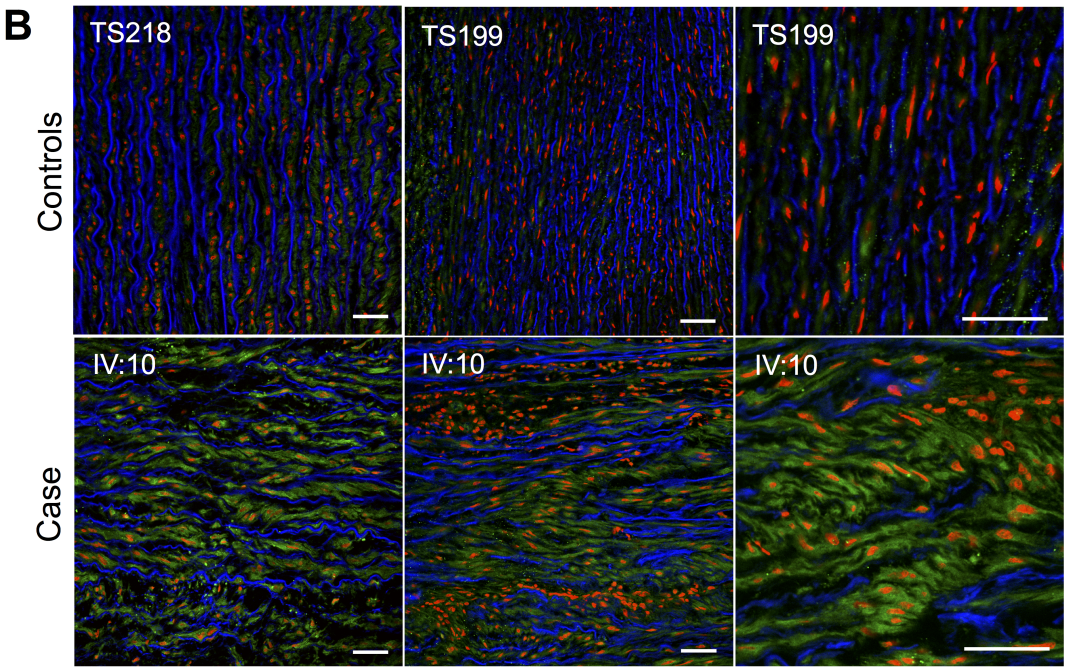
B
TS218
TS199
TS199
Controls
IV:10
IV:10
IV:10
Case